

Preparation and electrochemical properties of $\text{La}_{1.0}\text{Sr}_{1.0}\text{FeO}_{4+\delta}$ as cathode material for intermediate temperature solid oxide fuel cells

Jianhua Huang · Xiaoying Jiang · Xiaobo Li · Aiqin Liu

Received: 1 March 2008 / Accepted: 30 June 2008 / Published online: 23 September 2008
© Springer Science + Business Media, LLC 2008

Abstract Cathodic material $\text{La}_{1.0}\text{Sr}_{1.0}\text{FeO}_{4+\delta}$ for an intermediate temperature solid oxide fuel cell (IT-SOFC) was prepared via the glycine-nitrate process and characterized by X-ray diffraction (XRD), Fourier-transform infrared spectroscopy (FTIR), scanning electron microscopy (SEM). XRD results showed that no reaction occurred between the $\text{La}_{1.0}\text{Sr}_{1.0}\text{FeO}_{4+\delta}$ electrode and $\text{Sm}_{0.2}\text{Ce}_{0.8}\text{O}_{1.9}$ (SDC) electrolyte at 1000 °C. SEM results showed that the electrode formed good contact with the SDC electrolyte after sintering at 1000 °C for 2 h. The electrochemical properties of $\text{La}_{1.0}\text{Sr}_{1.0}\text{FeO}_{4+\delta}$ were measured using electrochemical impedance spectroscopy (EIS) and steady state polarization measurement. At 700 °C, the polarization resistance was about $3.90 \Omega\text{cm}^2$, and the lowest polarization overpotential was 57 mV at a current density of 55 mA cm^{-2} .

Keywords Solid oxide fuel cells · Cathode material · K_2NiF_4 -type structure · Electrochemical properties

1 Introduction

Solid oxide fuel cells (SOFCs) are prominent candidates of power generators that convert chemical energy directly with high efficiency into electricity while causing little pollution [1]. However, the technological development of SOFCs is limited due to their high operating temperature, typically around 900–1100 °C. In this temperature range, low-cost ferritic steel interconnectors can not be used and long-term

stability of the cell can not be improved as chemical reactions occur between electrodes and electrolyte. Reducing the operating temperature without a significant decrease in the power density appears to be the challenge of this technology [2, 3]. At low operating temperature, there are series of problems, one of major problems is the high polarization resistance of the cathode. Concerning the cathode material, using mixed ionic-electronic conductors appears to be a promising way to transform the triple-phase boundary (TPB) into a double contact (mixed conductor/gas phase), thus, lowering the cathode polarization [1, 4].

Recently, a new family of oxides with K_2NiF_4 -type structure (or A_2BO_4 structure) has been reported as a good mixed conductor material. Compared to the commonly used perovskite structured cathodes for SOFCs, K_2NiF_4 -type structure materials possess better thermal stability and smaller thermal-expansion coefficients ($10.5\text{--}14.2 \times 10^{-6} \text{ K}^{-1}$) [5–8] which match better with those of the commonly used electrolytes YSZ, GDC and SDC. Taking $\text{Ln}_2\text{NiO}_{4+\delta}$ (Ln=La, Pr, Nd) as examples, their surface oxygen exchange coefficients and oxide ion diffusivities are much higher than those of $\text{La}_{1-x}\text{Sr}_x\text{Fe}_{1-y}\text{Co}_y\text{O}_{3-\delta}$ [9, 10]. Presently, these oxides are extensively studied their possible usage as cathode materials for intermediate temperature solid oxide fuel cells (IT-SOFCs).

Among K_2NiF_4 -type structure materials for potential use as SOFC cathodes, $\text{Ln}_2\text{NiO}_{4+\delta}$ (Ln=La, Pr, Nd, Sm etc) based materials have attracted the most attention [11–16]. Another group of compounds that adopts the same structure and also contains excess oxygen is the $\text{La}_x\text{Sr}_{2-x}\text{FeO}_4$ phase. Jennings and Skinner suggested these materials as possible cathodes for SOFCs through a study of their thermal stability and conduction properties [17]. Omata has prepared and characterized $\text{La}_x\text{Sr}_{2-x}\text{FeO}_4$ and found single K_2NiF_4 -type structure phases for all compositions $x \geq 0.8$

J. Huang (✉) · X. Jiang · X. Li · A. Liu
College of Chemistry and Chemical Engineering,
Henan Institute of Science and Technology,
Hualan Road,
Xinxiang 453003, People's Republic of China
e-mail: hjhua@hist.edu.cn

[18]. However, Wang et al reported that the thermal-expansion coefficients of $\text{Ln}_{2-x}\text{Sr}_x\text{BO}_4$ ($\text{Ln}=\text{Pr}, \text{Sm}; \text{B}=\text{Fe}, \text{Ni}, \text{Co}, \text{Mn}$) would be increased with the improving of Sr-doping content [7]. Moreover, Li et al reported that $\text{Sm}_{1.0}\text{Sr}_{1.0}\text{NiO}_4$ showed the best electrochemical performance in $\text{Sm}_{2-x}\text{Sr}_x\text{NiO}_4$ family [16]. Thus, as a potential IT-SOFCs cathode material, $\text{La}_{1.0}\text{Sr}_{1.0}\text{FeO}_4$ has been synthesized and characterized, its electrochemical properties has also been investigated in the present study.

2 Experimental

2.1 Preparation and measurement of materials

The cathode material, oxide $\text{La}_{1.0}\text{Sr}_{1.0}\text{FeO}_{4+\delta}$ (abbreviated as LSF1010) was synthesized via the glycine-nitrate route [19]. Stoichiometric amounts of analytical grade $\text{La}(\text{NO}_3)_3 \cdot 6\text{H}_2\text{O}$, $\text{Sr}(\text{NO}_3)_2$ and $\text{Fe}(\text{NO}_3)_3 \cdot 9\text{H}_2\text{O}$ were dissolved and mixed in pure water, the concentration of total metal ions was 0.2 mol L^{-1} . Glycine was then added to the mixture in the molar ratio of 2:1 with respect to the total number of metal ions. The solution was heated to ignition on a hot plate to obtain a powder precursor. The precursor was calcined in air at 1000°C for 8 h. The electrolyte material, $\text{Sm}_{0.2}\text{Ce}_{0.8}\text{O}_{1.9}$ (SDC) powder was prepared using a citric-nitrate process and calcining at 800°C for 2 h [20]. The powder was then pressed into pellets in a stainless steel mold (13 mm in diameter) under about 300 MPa and sintered at 1400°C for 4 h.

The crystal structure of the powders was examined by X-ray diffraction (XRD) using a Bede D¹ X-ray diffractometer

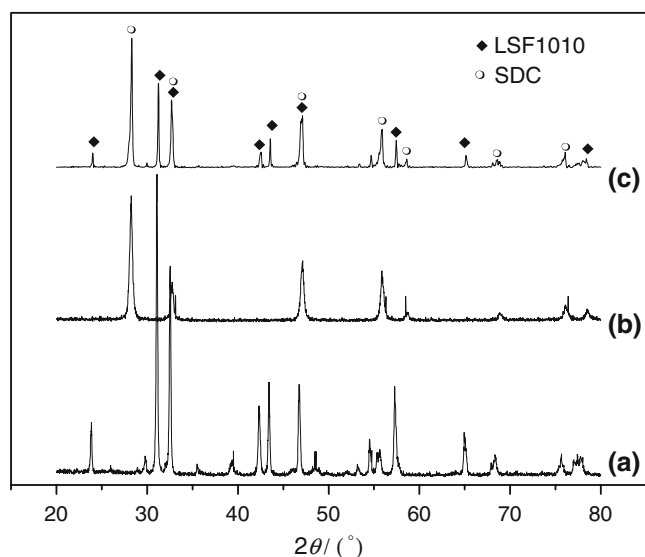


Fig. 1 XRD patterns of LSF1010 final powders (a); SDC final powders (b); LSF1010-SDC mixtures after sintered at 1000°C for 2 h (c)

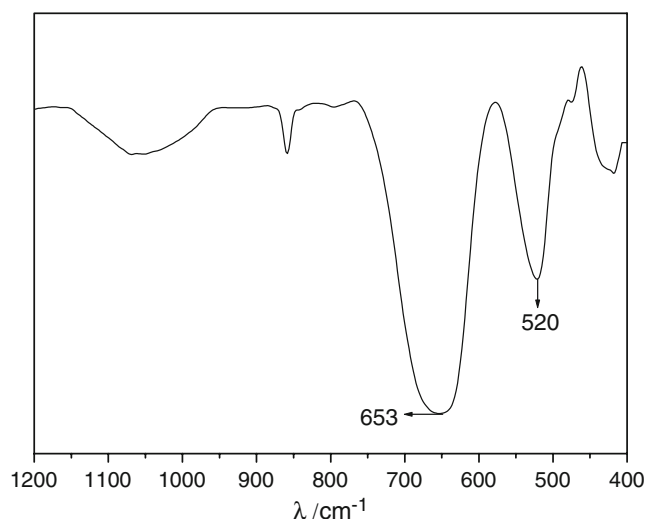


Fig. 2 FTIR spectrum of LSF1010 material sintered at 1000°C for 8 h in air

(Bede Scientific Ltd, UK) with $\text{Cu K}\alpha$ radiation operating at 40 kV, 45 mA; $\lambda=0.15418 \text{ nm}$. The diffraction angle was varied from 20° to 80° with a step of 0.02° and a scan rate of $1.2^\circ/\text{min}$. Fourier-transform infrared (FTIR) spectroscopy of the $\text{La}_{1.0}\text{Sr}_{1.0}\text{FeO}_{4+\delta}$ material sintered at 1000°C for 8 h in air was recorded on a PerkinElmer 1730 spectrophotometer in the mid-IR range from 4000 to 400 cm^{-1} with a resolution of 4 cm^{-1} using KBr pellets as standards. The microstructure of the sintered electrodes was examined with a Hitachi S-3000N scanning electron microscope.

2.2 Fabrication and measurement of half-cells and full-cells

A typical three-electrode method was used to investigate the electrochemical properties of the $\text{La}_{1.0}\text{Sr}_{1.0}\text{FeO}_{4+\delta}$ cathode on an SDC electrolyte in air. $\text{La}_{1.0}\text{Sr}_{1.0}\text{FeO}_{4+\delta}$ powder was mixed with an organic binder (ethyl cellulose,

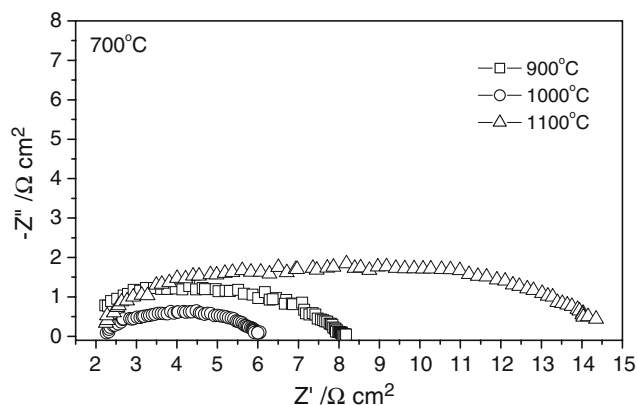
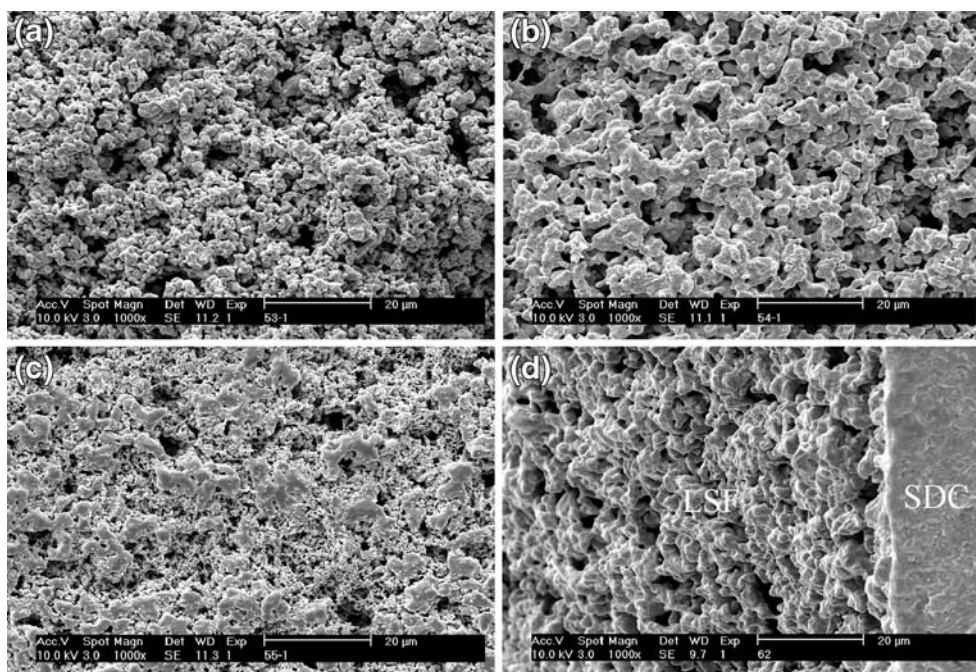


Fig. 3 Impedance spectrum of the LSF1010 cathode sintered at different temperatures for 2 h and then measured at 700°C in air

Fig. 4 SEM images of the LSF1010 electrode sintered at 900 °C (a); 1000 °C (b); 1100 °C (c) and the cross-section image of the test electrode(d)



α -terpineol) in a weight ratio of 1:1 to form a cathodic ink, which was subsequently painted on one side of an SDC pellet to form a working electrode (WE) with an effective area of 0.20 cm². After the cathode was sintered at 1000 °C for 2 h, Ag paste was painted on the other side of the SDC pellet, symmetrically opposite to the cathode as the counter electrode (CE). A silver reference electrode (RE) was attached to the same side of the WE by painting Ag paste on an uncoated region at the edge of the substrate. The distance between the edges of the RE and WE was about 3 mm. An Ag grid was printed on the surface of the cathode to serve as a current collector. Before testing, the half-cell was heated at 250 °C for 2 h [21] to remove organic solvents and binders. SDC electrolyte-supporting SOFCs were also prepared and tested using two-probe method. NiO and SDC powders were primarily mixed with a weight ratio of 50:50. The mixture was mixed with an organic binder (ethyl cellulose, α -terpineol) in a weight ratio of 1:1 to form an anode paste. The anode paste was painted on one side of SDC substrate and sintered at 1400 °C for 4 h. After that, the La_{1.0}Sr_{1.0}FeO_{4+ δ} cathode ink was screen printed on the other side of SDC substrate and sintered. Silver paste was used as seals of the SOFCs and silver wire as the conductor leading the current out [22, 23]. During electrochemical measurement of SOFCs, the cathode was exposed to ambient air, while the anode was exposed to fuel (pure hydrogen humidified with 3% vol water at 25 °C). The flow rate of the fuel was 50 sccm/ min.

Electrochemical impedance spectroscopy (EIS) and steady-state polarization measurement of the half-cell and the performance of the SDC electrolyte-supporting SOFCs

were carried out with an AUTOLAB PGStat30 electrochemical analyzer. For EIS measurement, the frequency ranged from 0.1 to 100 kHz and the AC amplitude was 5 mV. For steady-state polarization measurement of the half-cells, IR radiation was compensated.

3 Results and discussion

3.1 Characterization of powders

Figure 1(a) shows the XRD pattern of the final LSF1010 powders after calcination in air at 1000 °C for 8 h. It can be

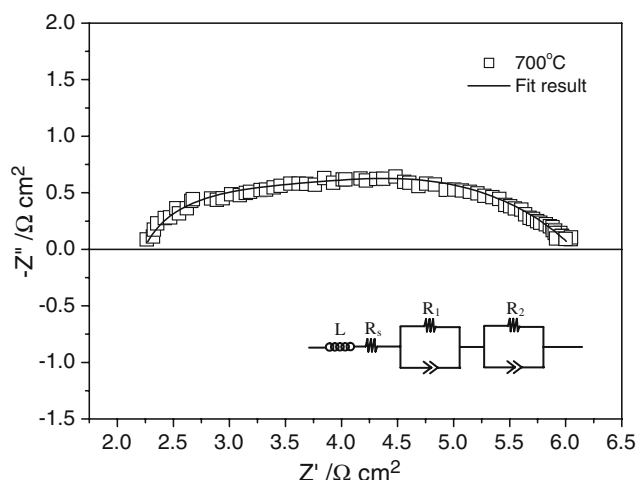


Fig. 5 Impedance spectrum for LSF1010 cathode at 700 °C under OCV condition

Table 1 Experimental data and fitting parameters extracted from EIS results at 700 °C.

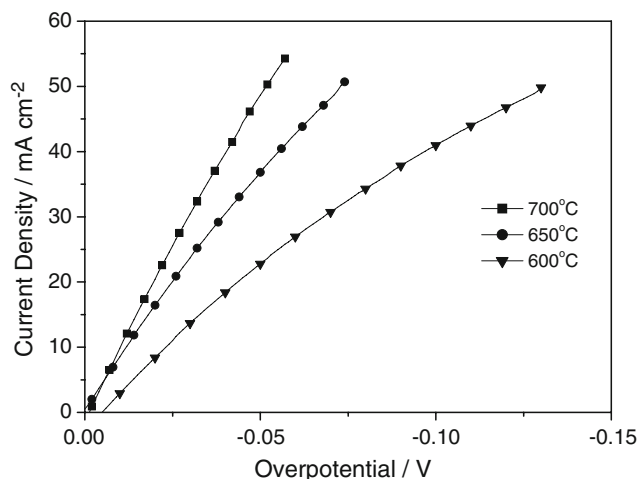
Parameters	L (H cm ²)	R _s (Ωcm ²)	R ₁ (Ωcm ²)	Q ₁ (Ω cm ² s ⁻ⁿ)	R ₂ (Ωcm ²)	Q ₂ (Ω cm ² s ⁻ⁿ)	R ₁ +R ₂ (Ω cm ²)
LSF1010	3.40×10 ⁻⁷	2.138	2.205	2.26×10 ⁻⁴	1.747	1.68×10 ⁻³	3.952

clearly observed that LSF1010 crystallized in a single phase with K₂NiF₄-type structure, and no impurities were found [17, 24, 25]. As we have known that reaction between the electrode materials and electrolyte is undesirable for the long-term stability of a SOFC. The reactivity of LSF1010 with the SDC electrolyte was further studied by mixing LSF1010 and SDC powders with a 1:1 weight ratio, and then sintering at 1000 °C for 2 h. From Fig. 1(c), it can clearly be seen that there is no new peaks other than those for LSF1010 and SDC, indicating that no reaction occurred. LSF1010 had good chemical compatibility with SDC electrolyte.

Figure 2 shows the FTIR spectra of the LSF1010 material sintered at 1000 °C for 8 h in air. In the finger range, the absorption peak at about 500 cm⁻¹ is assigned to the retractile vibration of A-O(II)-B bond in A₂BO₄ compound, and the absorption peak at about 650 cm⁻¹ is assigned to the retractile vibration of B-O bond in A₂BO₄ compound, which are characteristic absorption of A₂BO₄ materials in FTIR spectrum [8, 25, 26]. So, the FTIR results also showed that LSF1010 is a single K₂NiF₄-type structure phase.

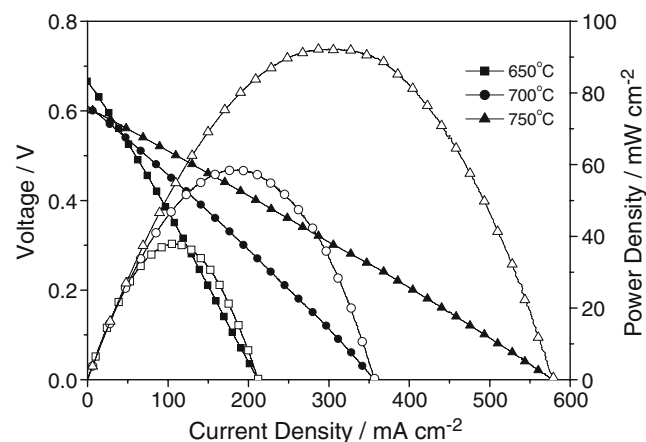
3.2 Sintering effects

In order to investigate the effect of sintering temperature on the properties of a LSF1010 cathode, different sintering conditions were studied. Figure 3 shows the impedance

**Fig. 6** Cathodic polarization curves for LSF1010 at different temperatures

spectroscopy of a LSF1010 cathode sintered at 900, 1000, and 1100 °C, respectively. The test was carried out at 700 °C in air on an SDC electrolyte. The intercepts of the impedance arcs on the real axis at high frequencies correspond to the resistance of the electrolyte and lead wires (R_s), while the overall size of the arcs is attributed to cathode polarization resistance (R_p). From the impedance spectra, it was seen that R_p was relatively large when the sintering temperature was low (900 °C). When the sintering temperature was 1000 °C, R_p decreased to its lowest value. R_p increased again when the sintering temperature was up to 1100 °C.

It is well known that the sintering temperature has a dramatic effect on the electrode microstructure, which in turn influences the electrode properties. Therefore, the microstructure of the sintered electrode at different temperatures was further studied. Figure 4 shows the SEM images of the surface of LSF1010 electrode sintered at 900 °C, 1000 °C and 1100 °C, respectively, for 2 h. It can be observed that the LSF1010 particle formed poor contacts with each other when the electrode was sintered at 900 °C for 2 h. Sintering at 1000 °C results in a structure with moderate porosity (Fig. 4(b)). However, a partial over-sintering phenomenon appears for the electrode sintered at 1100 °C. From Fig. 4(d), it can be seen that good contact formed between LSF1010 electrode and SDC electrolyte.

**Fig. 7** Cell voltages (solid symbols) and power densities (open symbols) as function of current density of SDC-supporting cell with LSF1010 cathode, measured in humidified H₂ and air in temperature range of 650–750 °C

3.3 Electrochemical performance

Electrochemical impedance spectroscopy under open-circuit-potential conditions was performed using three-electrode method for a LSF1010 cathode on an SDC electrolyte at 700 °C in air and the results are shown in Fig. 5. The associated electrical equivalent circuit is also reported (see inset Fig. 5), and the parameters values extracted from the EIS is presented in Table 1. A high-frequency inductive component (L) coming from the measuring system is visible at temperature above 650 °C; the series resistance, R_s , corresponds to the overall ohmic resistance from the electrolyte, electrodes and the connection wires; Q is the constant phase element, (R_{11}) and (R_{22}) correspond to the high- and low-frequency arcs, respectively [13]. The high-frequency arc (R_{11}) corresponds to charge transfer of oxygen ions at the electrode/electrolyte interface [27–29]. The low-frequency arc (R_{22}) reflects the oxygen adsorption or dissociation process [14]. The total polarization resistance (R_p) is the sum of R_1 and R_2 . It can be seen from Table 1 that R_1 is larger than R_2 , suggesting that O_2 reduction on the porous cathode is limited primarily by the charge-transfer process, presumably occurring at three phase boundary (TPB) [30]. The polarization resistance of LSF1010 cathode at 700 °C was about $3.9 \Omega \text{cm}^2$, similar to that of the reported $\text{La}_{1.6}\text{Sr}_{0.4}\text{NiO}_4$ and $\text{Sm}_{1.0}\text{Sr}_{1.0}\text{NiO}_4$ cathode materials [16, 31].

Figure 6 shows the cathodic polarization curve for LSF1010 cathode. It is clearly observed that the current density increases with increasing temperatures. The lowest polarization overpotential, 57 mV was measured for LSF1010 cathode at a current density of 55 mA cm^{-2} at 700 °C in air.

We applied the LSF1010 cathode to a SDC electrolyte-supporting SOFC. The curves of cell voltage and the corresponding power density versus current density are shown in Fig. 7. The cell shows encouraging performances with maximum output power densities of 92, 58, and 32 mW cm^{-2} at 750, 700, 650 °C, respectively.

4 Conclusions

The $\text{La}_{1.0}\text{Sr}_{1.0}\text{FeO}_{4+\delta}$ material was prepared via the glycine-nitrate process and its electrochemical properties as a potential cathode for IT-SOFC were measured. SEM results showed that a better microstructure formed when the electrode was sintered at 1000 °C for 2 h. The electrochemical impedance spectra revealed that $\text{La}_{1.0}\text{Sr}_{1.0}\text{FeO}_{4+\delta}$ materials had a similar electrochemical performance to that of the reported $\text{Ln}_{2-x}\text{Sr}_x\text{NiO}_4$ ($\text{Ln} = \text{La}, \text{Pr}, \text{Sm}$) materials. At 700 °C, the polarization resistance of $\text{La}_{1.0}\text{Sr}_{1.0}\text{FeO}_{4+\delta}$ is about $3.90 \Omega \text{cm}^2$, and the lowest polarization overpotential

is 57 mV at a current density of 55 mA cm^{-2} . The experimental results implied that the LSF1010 material can be considered as a potential cathodic material for the IT-SOFC.

References

- S.B. Adler, Chem. Rev. **4791**, 104 (2004)
- F. Mauvy, J.M. Bassat, E. Boehm, J.P. Manaud, P. Dordor, J.C. Grenier, Solid State Ion. **17**, 158 (2003)
- E. Ivers-Tiffée, A. Weber, D. Herbstritt, J. Eur. Ceram. Soc. **1805**, 21 (2001)
- J. Fleig, J. Maier, J. Eur. Ceram. Soc. **1343**, 24 (2004)
- S.J. Skinner, J.A. Kilner, Solid State Ion. **709**, 135 (2000)
- M.A. Daroukh, V.V. Vashook, H. Ullmann, F. Tietzb, I. Arual Raj., Solid State Ion. **141**, 158 (2003)
- Y.S. Wang, H.W. Nie, S.R. Wang, T.L. Wen, U. Guth, V. Valshook, Mater. Lett. **1174**, 60 (2006)
- C. Jin, J. Liu, Y.H. Zhang, J. Sui, W.M. Guo, J. Power Sources **482**, 182 (2008)
- E. Boehm, J.M. Bassat, M.C. Steil, P. Dordor, F. Mauvy, J.C. Grenier, Solid State Sci. **973**, 5 (2003)
- E. Boehm, J.M. Bassat, P. Dordor, F. Mauvy, J.C. Grenier, P. Stevens, Solid State Ion. **2717**, 176 (2005)
- N. Solak, M. Zinkevich, F. Aldinger, Solid State Ion. **2139**, 177 (2006)
- M.L. Fontaine, C. Laberty-Robert, F. Ansart, P. Tailhades, J. Power Sources **33**, 156 (2006)
- V. Vashook, J. Zosel, T.L. Wen, U. Guth, Solid State Ion. **1827**, 177 (2006)
- F. Mauvy, J.M. Bassat, E. Boehm, J.P. Manaud, P. Dordor, J.C. Grenier, Solid State Ion. **17**, 158 (2003)
- C. Lalanne, F. Mauvy, E. Siebert, M.L. Fontaine, J.M. Bassat, F. Ansart et al., J. Eur. Ceram. Soc. **4195**, 27 (2007)
- Q. Li, Y. Fan, H. Zhao, L.P. Sun, L.H. Huo, J. Power Sources **64**, 167 (2007)
- A.J. Jennings, S.J. Skinner, Solid State Ion. **663**, 152–153 (2002)
- T. Omata, K. Ueda, N. Ueda, M. Katada, S. Fujitsu, T. Hashimoto et al., Solid State Commun. **807**, 88 (1993)
- L.A. Chick, L.R. Pederson, G.D. Maupin, J.L. Bates, L.E. Thomas, G.J. Exarhos, Mater. Lett. **6**, 10 (1990)
- D.H.A. Blank, H. Kruidhof, J. Flokstra, J. Phys. D. Appl. Phys. (Berl.) **226**, 21 (1988)
- C. Jin, J. Liu, W.M. Guo, Y.H. Zhang, J. Power Sources **506**, 183 (2008)
- J. Liu, S.A. Barnett, Solid State Ion. **11**, 158 (2003)
- J. Liu, Z. Lü, S.A. Barnett, Y. Ji, W.H. Su, the 9th International Symposium on Solid oxide Fuel Cells Electrochemical Society Proceedings. 1976, 07 (2005)
- D.C. Zhu, X.Y. Xu, S.J. Feng, W. Liu, C.S. Chen, Catal. Today **151**, 82 (2003)
- C. Li, T.H. Hu, H. Zhang, Y. Chen, J. Jin, N.R. Yang, J. Membr. Sci. **1**, 226 (2003)
- J.W.J. Potts, Chemical Infrared Spectroscopy, vol. **135** (Wiley, New York, 1963), p. 1
- V.V. Vashook, S.P. Tolochko, I.I. Yushkevich, L.V. Makhnach, I.F. Kononyuk, H. Altenburg et al., Solid State Ion. **245**, 110 (1998)
- K. Ishikawa, S. Kondo, H. Okanc, S. Suzuki, Y. Suzuki, Bull. Chem. Soc. Jpn. **1295**, 60 (1987)
- L.A. Chick, L.R. Pederson, G.D. Maupin, J.L. Bates, L.E. Thomas, G.J. Exarhos, Mater. Lett. **6**, 10 (1990)
- S.B. Adler, Solid State Ion. **125**, 111 (1998)
- Q. Li, Y. Fan, H. Zhao, L.H. Huo, Chin J. Inorg. Chem **2025**, 22 (2006)